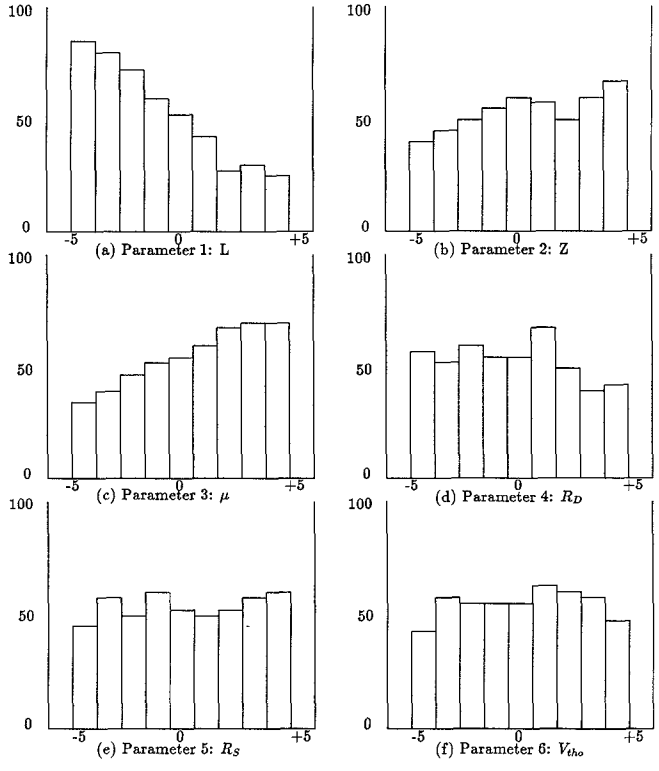

Fig. 6. Yield factor histograms, yield% versus parameter% of complementary HEMT inverter chain.

TABLE III
YIELD SENSITIVITY OF HEMT INVERTER CHAIN WITH COMPLEMENTARY LOGIC

Parameter	Yield Sensitivity (yield%/parameter%)
Parameter 1 : L	-7.56 ± 0.49
Parameter 2 : Z	$+2.25 \pm 0.54$
Parameter 3 : μ	$+4.12 \pm 0.29$
Parameter 4 : R_D	-1.62 ± 0.87
Parameter 5 : R_S	$+0.86 \pm 0.62$
Parameter 6 : V_{tho}	$+0.62 \pm 0.71$

capacitor C5. Here also we have used the TRW #2078 HEMT's for both p- and n-channel HEMT's.

For the inverter chain, we have chosen the risetime of the output at C5 as the performance specification. The risetime is defined as the time taken by the output signal to rise from 10% to 90% of its final steady state in response to a step voltage applied at the input. For this circuit, the risetime is specified to be less than 16.85 psec.

1000 simulations were performed for the inverter chain. In Fig. 6, we present the yield factor histograms of this circuit. The yield sensitivities were calculated and are given in Table III. For this circuit, we observed similar results as the NOR gate. But in this case, the yield sensitivity with respect to L, Z and mobility is less as compared to example I. Again the yield is almost insensitive to R_D, R_S and V_{tho} of the device.

VI. Conclusion

This work uses the yield factor histograms to study the yield and the yield sensitivity of HEMT circuits with process parameter variations. From our statistical Monte Carlo analysis of two example circuits, we observed that the yield is sensitive to the device dimension and to the carrier mobility and almost insensitive to the threshold voltage.

The analysis technique we present in this paper will help the microwave circuit designer to efficiently calculate yield sensitivity to process parameter variations.

Acknowledgment

The authors would like to thank the NASA Space Engineering Research Center, University of Idaho for partial funding. The second author acknowledges Jesus of Nazareth for His sacrifice and example.

References

[1] J. E. Purviance and M. D. Meehan, "A sensitivity figure for yield improvement," *IEEE Trans. Microwave Theory Techniques*, vol. 36, pp. 413–417, Feb. 1988.
[2] J. C. Sarker and J. E. Purviance, "Yield sensitivity study of AlGaAs/GaAs high electron mobility transistor," *Int. J. Microwave and Millimeter-Wave Computer-Aided Engineering*, vol. 2, pp. 12–27, Jan. 1991.
[3] G. W. Wang ang W. H. Ku, "An analytical and computer-aided model of the Al-GaAs/GaAs high electron mobility transistor," *IEEE Trans. Electron Devices*, vol. ED-33, pp. 657–663, May 1986.
[4] J. C. Sarker and J. E. Purviance, "DC and small-signal physical models for the al-GaAs/GaAs high electron Mobility transistor," in *Proc. 3rd NASA Symp. VLSI Design*, Moscow, ID, Oct. 1991.
[5] A. MacFarland, J. E. Purviance, D. Loescher, K. Diegert, and T. Ferguson, "Centering and tolerancing the components of microwave amplifiers," in *IEEE MTT-S Int. Microwave Symp. Dig.*, June 1987, pp. 633–636.
[6] F. N. Trofimenkoff, "Field-dependent mobility analysis of the field-effect transistor," in *Proc. IEEE*, vol. 53, pp. 1765–1766, Nov. 1965.
[7] K. Hilosaka, Y. Hirachi, T. Mimura, and M. Abe, "A Microwave power double-heterojunction high electron mobility transistor," *IEEE Electron Device Lett.* vol. EDL-6, pp. 341–343, July 1985.
[8] S. M. Liu, M. B. Das, W. Kopp, and H. Morkoc, "Determination of 2-D electron-gas carrier mobility in short gate-length MODFET's by direct elimination of parasitic resistance effects." *IEEE Electron Device Lett.*, vol. EDL-6, pp. 594–596, Nov. 1985.
[9] M. Meehan and T. Wandinger, "Accurate design centering and yield prediction using the truth model," in *IEEE Microwave Theory Tech. Symp. Dig.*, June 1991, pp. 1201–1204.
[10] D. E. Fulkerson, "Feedback FET logic: a robust, high-speed, low-power GaAs logic family," *IEEE J. Solid-State Circuits*, vol. 26, pp. 70–74, Jan 1991.
[11] M. Shur, *GaAs Devices and Circuits*. New York: Plenum, 1987.

Analytic Physics-Based Expressions for the Empirical Parameters of the Statz–Pucel MESFET Model

S. D'Agostino, G. D'Inzeo, P. Marietti, L. Tudini, and A. Betti-Berutto

***Abstract*—In this paper we present a novel approach to the evaluation of the dc parameters of a semi-empirical MESFET model: starting from the analytical expression of the drain current derived from a physics-based model, previously proposed, we provide a method to calculate**

Manuscript received August 6, 1991; revised January 23, 1992.
The authors are with the Department of Electronic Engineering, University "La Sapienza" of Rome, Via Eudossiana 18, 00184 Rome, Italy.
IEEE Log Number 9200767.

the empirical dc parameters of the so called "Raytheon" model. The comparison between computed and measured dc characteristics is quite satisfactory on GaAs microwave FET's of 1 μm or more gate length. By adding to the results, obtained in this work, an adequate model of the stray capacitances, the circuit performance can be optimized using the technological characteristics of active devices.

NOMENCLATURE

a	Active-layer thickness.
E_s	Electric field value at the electron drift velocity saturation.
v_s	Saturation velocity.
f_{CLM}	Channel length modulation factor.
g_0	Conductance of the metallurgical channel.
$I_{P\,\mathrm{sat}}$	Saturation current of physical model.
$I_{R\,\mathrm{sat}}$	Saturation current of Raytheon model.
K_d	Domain parameter.
L	Gate length.
L_1	Shockley region's length.
L_{sat}	Length of velocity saturation region under the gate.
L_s	Saturation region's length.
N_D	Doping density of the active zone.
ϵ	Dielectric permittivity.
q	Electronic charge value.
V_{bi}	Built-in voltage of Schottky contact.
V_p	Voltage drop across non-saturated region under the gate.
V_{po}	$= qa^2N_D/2\epsilon$ ideal pinch-off voltage.
V_T	Threshold voltage of the MESFET.
Z	Gate width.
μ_0	Low-field electron mobility.

I. INTRODUCTION

Microwave circuit simulation programs are useful and fast tools, especially if circuits consist of a large number of components. Such tools (namely MWSPICE™ [1], LIBRA™ [2], etc.) can work with semi-empirical models or with physical models or, in some case, with both.

If the technological process is, at least in part, under control (as in the case of MMIC design [3]), the physical model is the best approach to the design. Otherwise, as in the case of hybrid design, it is sufficient to refer to semi-empirical models [4], [5], whose parameters are derived from measurements.

Clearly the semi-empirical model is more convenient from the computational complexity point of view. On the other hand, it is also clear that a physical model gives a more tight insight into circuit performances. It would be useful to make the two models interact in such a way as to derive the semi-empirical model parameters directly from the physical model.

In this work, we show that it is possible to give the most meaningful dc elements of the semi-empirical MESFET model a functional dependence on the physical structure of the device. This approach is very useful in optimization procedures, that are more efficient if carried out by a designer who knows the relations between the elements of the equivalent circuit and the physical-geometrical parameters. To obtain the analytical expressions, we started from the already known analytic physical models whose validity is the basis of this work.

In Sec. II we discuss the most used semi-empirical models.

In Sec. III we recall the fundamental points of the theory, leading to the physical models as found in current literature.

In Sec. IV we obtain analytic physics-based expressions of the "Raytheon" model parameters.

In Sec. V we discuss the experimental results.

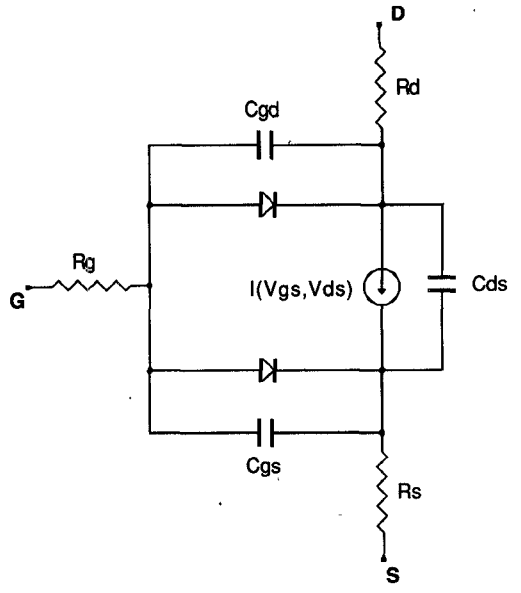

Fig. 1. The large signal equivalent circuit of the Raytheorn model.

II. LARGE SIGNAL EQUIVALENT CIRCUITS

The first, though incomplete, large signal equivalent circuit of the MESFET was proposed by Rauscher and Willing in the late 1970s [6]. In 1980, the Curtice model [4] was the first equivalent circuit expressly conceived to be used in time-domain circuit simulation programs as SPICE™. In this model, the non-linear elements do have an analytic functional expression and this simplifies the fitting of the circuit parameters.

The Curtice model presents two problems. First, the square law variation of I_d versus V_{gs} in the saturation region, derived from the Si JFET model, describes precisely only MESFET's with low pinch-off voltage; for devices that do not fulfil this hypothesis, the square law is valid only near the pinch-off. Second, the C_{gs} and C_{gd} capacitances were used asymmetrically and with a C_{gd} constant with respect to the bias, reflecting the actual situation only in the saturation region.

In 1987, the above-mentioned problems were solved with the model (Fig. 1) proposed by Statz *et al.*, usually known as "Raytheon model" [5], which has the same topology as the Curtice model, with the addition of a gate-drain diode and a nonlinear C_{gd}. For the saturation current, the following expression is used:

$$I_{\mathrm{sat}} = \frac{\beta(V_{gs} - V_T)^2}{1 + b(V_{gs} - V_T)}. \tag{1}$$

Equation (1) introduces a new parameter b; for small values of $V_{gs} - V_T$, i.e. near the pinch-off, the expression follows a square law, whereas for high values of $V_{gs} - V_T$ the behavior is linear in $V_{gs} - V_T$. The channel length modulation is given by the term $(1 + \lambda V_{ds})$, while, in the region before saturation, a polynomial expression is used, with a hyperbolic tangent like behavior. The expressions describing the capacitance behavior are rather complex because they consider the various bias conditions: however, they describe a progressive transition from saturation to $V_{ds} = 0$, and in the inverse connection the role of C_{gs} and C_{gd} is reversed [5].

Though other analytical MESFET models have been proposed, trying to solve the same problems of Curtice model [7], [8] and other anomalous effects [9], [10], the Raytheon model results accurate and with a good structure; in fact, it was incorporated in SPICE.

In this model there are some empirical parameters (i.e., α, β, λ, b), for which we obtain analytical expressions, starting from the physical characteristics of the components. The approach used is based on the gradual channel approximation and a piecewise linear approximation for the electron velocity, hence, at first glance, it is suitable only for gate lengths greater than 1 μm. However, recent works [11], [12] have shown that such approximations turn out to be valid for ultra-short gates (80 ÷ 100 nm) [13], when velocity saturation, overshoot effects [14], and fringing effects [11] are included.

III. The $I_D(V_{gs}, V_{ds})$ Characteristic

A. The Physical Model

In Fig. 2(a) and (b) the well-known situations of a self-aligned and a non self-aligned MESFET are shown: in region I the gradual channel approximation is used and the mobility is assumed to be a constant value μ_o; in region II (and III) the saturation velocity (v_s) is reached [15]. For simplicity sake, we assume a uniform channel doping profile N_D.

It is possible to have an analytical solution for L_s (Fig. 2(a) and (b)) and then for $L_1 = L - L_s$ [15]:

$$L_s(V_{ds}, V_{gs}) = \frac{2a}{\pi} \sinh^{-1}\left\{\frac{\pi K_d}{2aE_s}[V_{ds} - V_p(V_{gs})]\right\} \tag{2}$$

where K_d is the domain parameter [15] and V_p is the voltage drop between the point $x = 0$ and $x = L_1$. After some mathematical manipulation on the drain-current expression of the square-law model [15] we obtain:

$$I_d(V_{gs}, V_{ds}) = \frac{q\mu_o N_D Z a E_s}{V_{po}[V_{po} + 3E_s L]}(V_{gs} - V_T)^2 \cdot \frac{V_{po} + 3E_s L}{V_{po} + 3E_s[L - L_s]} \tag{3}$$

where the third factor is the channel length modulation factor, that will be called f_{CLM}, whereas the product between the first two factors is equal to the current value for $V_{ds} = V_p$, namely I_p. Taking into account (2), we can write:

$$I_d(V_{gs}, V_{ds}) = I_p(V_{gs})\, f_{CLM}(V_{ds}, V_{gs}) \tag{4}$$

which is a new general expression where I_p represents the current at the onset of saturation velocity ($L_s = 0$) and it is a true function of V_{gs} without necessarily being a square law. Equations (3) and (4) above allow us to handle a mathematical model directly related to FET physical parameters.

B. The Statz et al. Model (Raytheon Model)

The analytical expression of I_{d_R} in the Raytheon model [5] (R stands for Raytheon) is

$$I_{d_R}(V_{gs}, V_{ds}) = \frac{\beta(V_{gs} - V_T)^2}{1 + b(V_{gs} - V_T)} P(\alpha, V_{ds})(1 + \lambda V_{ds}) \tag{5}$$

where

$$P(\alpha, V_{ds}) = \begin{cases} 1 - \left(1 - \alpha\dfrac{V_{ds}}{3}\right)^3 & \text{for } 0 < V_{ds} < 3/\alpha \\ 1 & \text{for } V_{ds} \geq 3/\alpha. \end{cases} \tag{6}$$

According to the properties of $P(\alpha, V_{ds})$, we can note that the first factor in (5) represents the saturation current value, after which the current doesn't further increase (neglecting the influence of the output conductance) although V_{ds} increases. Such a current will be called $I_{R\,sat}$. For $V_{ds} = 3/\alpha$, $P(\alpha, V_{ds})$ is equal to 1; we call this voltage value V_{sat}.

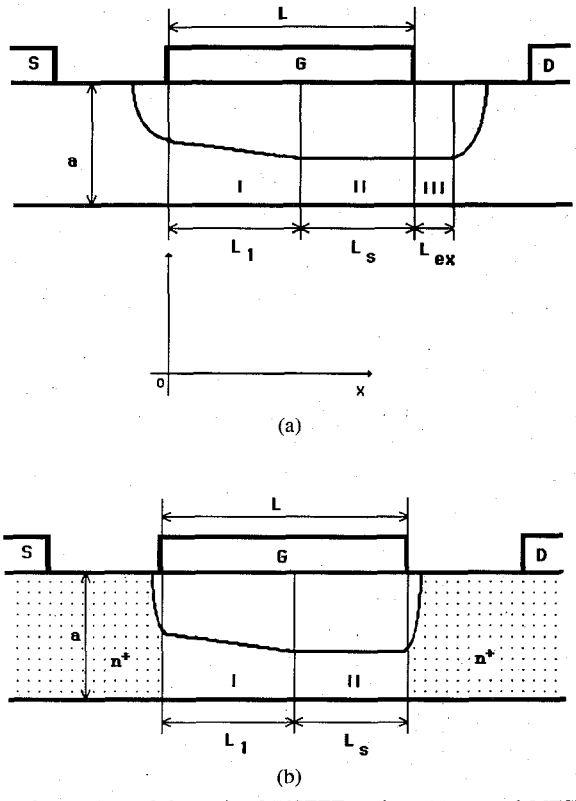

Fig. 2. Cross view of the active MESFET region: (a) normal MESFET. (b) self-aligned MESFET.

IV. Analytic Physics-Based Expressions of the Raytheon Model Parameters

Clearly $I_{R\,sat}$ and I_p of the physical model do not represent the same quantity. I_p is the current at the onset of the velocity saturation ($L_s = 0$), meanwhile $I_{R\,sat}$ is the current for $V_{ds} = 3/\alpha$. Neglecting this difference can cause a considerable error: a connection between (4) and (5) can be set up only after defining a saturation current $I_{P\,sat}$ (where P stands for physical) also for the physical model. Later on we will come back to this matter: at the moment we consider V_{sat} a known value. Hence, $I_{P\,sat}$ is (4):

$$I_{P\,sat}(V_{gs}) = I_p(V_{gs})\, f_{CLM}(V_{sat}, V_{gs}) \tag{7}$$

where $f_{CLM}(V_{sat}, V_{gs})$ is derived by replacing, in the third factor of (4), the value of L_s given by (2) with $V_{ds} = V_{sat}$. In reality, this value depends on V_{gs}. We have found, however, that L_s is quite independent of V_{gs} for $V_{ds} > E_s L/V_{po}$, that is our case. Therefore we can choose for V_{gs} the built-in value V_{bi}, obtaining:

$$L_{sat} = L_s(V_{gs} = V_{bi}, V_{ds} = V_{sat}) \tag{8}$$

Using this value, we can determine f_{CLM} as

$$f_{CLMsat} = \frac{V_{po} + 3E_s L}{V_{po} + 3E_s(L - L_{sat})} \tag{9}$$

which turns out to be independent of V_{gs}. Then (7) becomes:

$$I_{P\,sat}(V_{gs}) = I_p(V_{gs}) f_{CLMsat}. \tag{10}$$

The simplification introduced in (8) allows us to make a comparison between $I_{R\,sat}$ and $I_{P\,sat}$, from which it will be possible to

obtain the requested link between β and b of the Raytheon model and the physics-geometrical parameters of the device.

A. Determination of β and b

As $I_p(V_{gs})$ is the current at the onset of velocity saturation, that is for $E = E_s$ at $x = L$, we have [16]:

$$I_p(s) = g_o V_{po}\xi\left[1 - \sqrt{\frac{s^4 - s^2 - \xi}{s^2 - (1 + \xi)}}\right] \tag{11}$$

where s is the depleted fraction in the channel at point $x = 0$, $g_o = q\mu_o N_D Za/L$ is the so-called conductance of the metallurgical channel and ξ is the saturation index [11]. It would be better to turn $I_{R\,sat}$, given by the first factor of (5), into an expression including s instead of V_{gs}. After some algebra one obtains:

$$I_{R\,sat}(s) = \frac{-\beta V_{po}}{b}\frac{(s^2 - 1)^2}{s^2 - \left(1 + \dfrac{1}{bV_{po}}\right)}. \tag{12}$$

We want to find values for β and b as a function of g_o, ξ, V_{po}, etc. in such a way as to make the functions $I_{R\,sat}(s)$ and $I_{P\,sat}(s)$ as similar as possible. A matching between the two curves has to be carried out by considering the more or less great importance of the various zones of the curves. The two curves always meet at $s = 1$ where they must be equal to zero (pinch-off situation). We impose a first crossing point between the two current curves at $s = 0$. If we consider the great importance of the zone between 0.5 and 1, a second matching point can be positioned at about $s = 0.7$.

For $s = 0.7$ the factor $1/(bV_{po})$, in $I_{R\,sat}$, equals $(1 + \xi^2)$, and we obtain the requested value b as a function of the physical-geometrical parameters:

$$b = \frac{1}{V_{po}(1 + \xi^2)}. \tag{13}$$

By substituting (13) into (12) and making the resulting expression equal to $[f_{CLMsat} I_p(s)]$, with $s = 0$, we have the requested expression of β, that is

$$\beta = \frac{g_o}{V_{po}} f_{CLMsat}\frac{\xi\left(1 - \sqrt{\dfrac{\xi}{1 + \xi}}\right)(2 + \xi^2)}{1 + \xi^2}. \tag{14}$$

An example of the matching obtained is given in Fig. 3, where $\xi = 0.15$.

B. Determination of α

In the Raytheon model α is the parameter that describes the behavior of the curves $I_{dR}(V_{gs}, V_{ds})$ in the region before the current saturation; thus it has a double function. First α is just the slope of $P(\alpha, V_{ds})$ at $V_{ds} = 0$. Secondly, for $V_{ds} = 3/\alpha$ the I_d/V_{ds} curve ((5) and (6)) becomes flat and $3/\alpha$ may be considered the right value of V_{sat} in the Raytheon model. Therefore, the exactness of the modeling of both these quantities is based on the goodness of the polynomial form that is chosen empirically to represent the MESFET behavior.

Now we try to find an expression for α so that, once it has been put into $I_{R\,sat}$, it may give the same slope (for V_{ds} approaching 0) as that obtained from the physical model. That implies the condition:

$$\lim_{V_{ds}\to 0}\frac{\partial I_d}{\partial V_{ds}} = \lim_{V_{ds}\to 0}\frac{\partial I_{dR}}{\partial V_{ds}}. \tag{15}$$

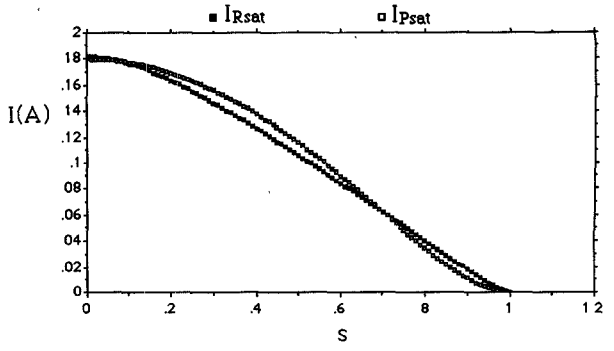

Fig. 3. Comparison between the current of Raytheon and physical models.

The physical model valid in this region is the Schockley's [17] and then from (15) we obtain:

$$\alpha = \frac{V_{po} + 3E_s\left[L - \dfrac{2a}{\pi}\sinh^{-1}\left(\dfrac{\pi K_d}{2aE_s}\right)\right]}{E_s L\left(1 - \sqrt{\dfrac{E_s L}{V_{po} + E_s L}}\right)(V_{po} + 3E_s L)}. \tag{16}$$

We can now evaluate $V_{sat} = 3/\alpha$, which we have supposed as known in (8) and include its value in (9) and (14) for the final determination of β.

C. Determination of λ

In the Raytheon model the output conductance is described by the multiplicative factor $(1 + \lambda V_{ds})$. As $V_{ds} > 3/\alpha$, I_{dR} becomes:

$$I_{dR}(V_{gs}, V_{ds}) = I_{R\,sat}(V_{gs})(1 + \lambda V_{ds}). \tag{17}$$

In the physical model, the channel length modulation is the phenomenon determining the output conductance of the inner MESFET: it has a vaguely logarithmic behavior (owing to the $\sinh^{-1}$ included in L_s) and presents a variable slope. Therefore a straight line will never represent such a behavior completely, but can only approximate it. For this approximation, we use a secant straight line that supplies a minimum total error compared with the original curve in the zone of greater interest for the device behavior. In this way we have obtained:

$$\lambda = \frac{\dfrac{V_{po} + 3E_s(L - L_{sat})}{V_{po} + 3E_s[L - L_s(2V_{po} + E_s L/1 + \xi, V_{bi})]} - 1}{2V_{po} + \dfrac{E_s L}{1 + \xi}} \tag{18}$$

where L_{sat} is given by (8) and (16) and $L_s(V_{ds}, V_{gs})$ by (2).

V. Experimental Results

As new expressions for the empirical parameters of the Raytheon model have been obtained, it is necessary to check their validity.

As already mentioned, the Raytheon model is used in many SPICE versions. Once the parameters are obtained by means of the previous equations (see Table II), it is possible to obtain the characteristic $I_d - V_{ds}$ for various gate voltages. We used our formulas to simulate the behavior of several MESFET's. A good agreement between measurements and theory has been generally obtained. In particular, we show here the curves (Figs. 4 and 5) resulting from the simulation and the data measurements of two very different MESFET's [15] whose parameters are shown in Table I. In Table II, the parameters derived by using (13), (14), (16), and (18) are reported.

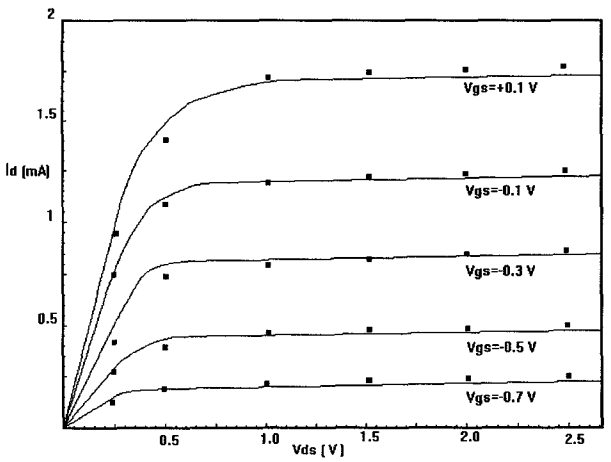

Fig. 4. The obtained I–V characteristic of a low pinch-off MESFET (FET 1) [15] (solid line = this work, square = measured data).

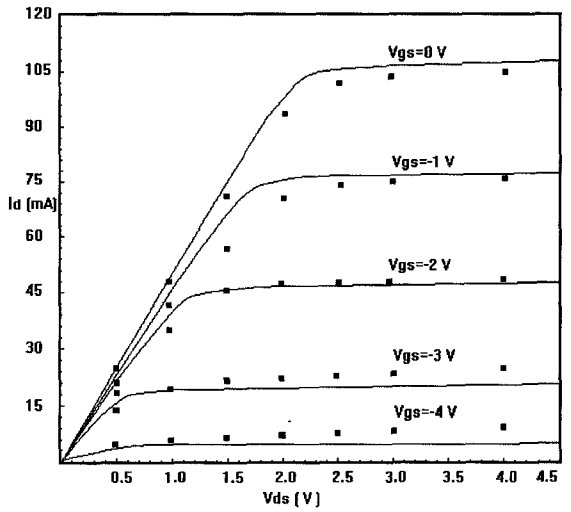

Fig. 5. The obtained I–V characteristic of a high pinch-off MESFET (FET 2), [15] (solid line = this work, square = measured data).

TABLE I
PHYSICAL PARAMETERS OF THE TWO MESFET

	FET 1	FET 2	
V_{po}	1.8	5.3	V
N_d	1.81 10^{17}	6.5 10^{16}	Atoms/cm^3
L	1.3	1	μm
Z	200	500	μm
V_{bi}	0.76	0.75	V
v_s	1.2 10^5	1.2 10^5	m/s
μ_o	0.306	0.45	m^2/Vs
R_s	6.8	16.5	Ω
R_d	68	11.3	Ω
K_d	0.1	0.1	

TABLE II
OBTAINED PARAMETERS

FET 1	FET 2	
α 4.07	4.3	1/V
β 0.00235	0.0129	A/V^2
λ 0.0158	0.0164	1/V
b 0.528	0.188	1/V

Considering the statistical variations of technological parameters, the theoretical simplification and the approximation of measurements, the results obtained in this work agree quite well with the available experimental data.

VI. CONCLUSION

In this work, we have obtained analytical expressions for the empirical parameters of the Raytheon model: α, b, λ, β. Theoretical and experimental results for the I–V characteristics of different devices are in good agreement. The approach presented is based on the gradual channel approximation, hence it has a validity only for MESFET's with $L \geq 1$ μm. This means that the results obtained in this work would seem to be limited in practice as all the up-to-date available MESFET's have submicron gate length [19]–[21]. Further work is in progress, to apply a similar approach to submicron MESFET's, including surface-depletion effects [9], non abrupt depletion region interface [19], carrier injection in the buffer layer [22].

It is of remarkable interest that, as it has been experimentally demonstrated [11], the gradual channel approximation turns out to be again valid for ultra-short-gate (80 ÷ 100 nm) length MESFET's, if velocity saturation in the whole channel, overshoot effect, and fringing effects are included.

REFERENCES

[1] *Microwave SPICE-User's Guide*, EEsof, 1991.
[2] *Touchstone & Libra-Utilities*, EEsof, 1991.
[3] P. Ladbrooke, *MMIC Design: GaAs FETs and HEMTs*. Norwood, MA: Artech House, 1989.
[4] W. R. Curtice, "A MESFET model for use in the design of GaAs Integrated Circuits," *IEEE Trans. Microwave Theory Tech.*, vol. MTT-28, no. 5, pp. 448–456, Sept. 1980.
[5] H. Statz, R. A. Pucel, and H. A. Haus, "GaAs FET device and circuit simulation in SPICE," *IEEE Trans. Electron Devices*, vol. ED-34, no. 2, pp. 160–169, Feb. 1987.
[6] C. Rauscher and H. A. Willing, "Quasi-static approach to simulating nonlinear GaAs FET behavior," in *Proc. IEEE MTT-S Int. Microwave Symp. Dig.*, Orlando, 1979, pp. 402–404.
[7] W. R. Curtis and M. Ettemberg, "A nonlinear GaAs FET model for use in the design of output circuits for power amplifiers," *IEEE Trans. Microwave Theory Tech.*, vol. MTT-33, pp. 1383–1394, 1985.
[8] J. M. Golio, *Microwave MESFETs & HEMTs*. Norwood, MA: Artech House, 1991, pp. 139–140.
[9] P. H. Ladbrooke and S. R. Blight, "Low-field low-frequency dispersion of transconductance in GaAs MESFET's with implications for other rate-dependent anomalies," *IEEE Trans. Electron Devices*, vol. 35, no. 3, pp. 257–267, Mar. 1988.
[10] P. Pouvil, J. L. Gautier, and D. Pasquet, "A new analytical model for the GaAs MESFET in the saturation region," *IEEE Trans. Electron Devices*, vol. 35, no. 8, pp. 1215–1222, Aug. 1988.
[11] G. Bernstein, D. K. Ferry, "Velocity overshoot in ultra-short-gate-length GaAs MESFET's," *IEEE Trans. Electron Devices*, vol. 35, no. 7, pp. 887–892, July 1988.
[12] P. C. Chao, M. S. Shur *et al.*, "DC and microwave characteristics of sub-0.1-μm gate-length planar-doped pseudomorphic HEMT's," *IEEE Trans. Electron Devices*, vol. 36, no. 3, pp. 461–473, Mar. 1989.
[13] J. A. Adams *et al.*, "GaAs MESFET's with gate lengths from 250 down to 30 nm: characterization at microwave frequencies," *IEEE Trans. Electron Devices*, vol. 38, no. 10, Nov. 1989.
[14] M. S. Shur and L. F. Eastman, "Ballistic transport in semiconductors at low temperatures for low-power high-speed logic," *IEEE Trans. Electron Devices*, vol. ED-26, no. 11, pp. 1677–1683, Nov. 1979.
[15] M. S. Shur, "Analytical model of GaAs FET's," *IEEE Trans. Electron Devices*, vol. ED-32, no. 1, pp. 70–72, Jan. 1985.
[16] R. A. Pucel, H. A. Statz, and H. Haus, "Signal and noise properties of gallium arsenide microwave field-effect transistors," in *Advances in Electronics and Electron Physics*, vol. 38. New York: Academic Press, 1975, pp. 195–205.

[17] M. S. Shur, "Analytical model of GaAs MESFET's," *IEEE Trans. Electron Devices*, vol. ED-25, no. 6, pp. 612–618, June 1978.
[18] ——, "Low field mobility, effective saturation velocity and performance of submicron GaAs MESFET's," *Electron. Lett.*, vol. 18, no. 21, pp. 909–911, Oct. 1982.
[19] C. M. Snowden and R. Pantoja, "Quasi-two-dimensional MESFET simulation for CAD," *IEEE Trans. Electron Devices*, vol. 36, no. 9, pp. 1564–1573, Sept. 1989.
[20] M. Ali Khatibzadeh and R. J. Trew, "A large-signal, analytical model for the GaAs MESFET," *IEEE Trans. Microwave Theory Tech.*, vol. 36, pp. 231–238, Feb. 1988.
[21] C. S. Chang *et al.*, "GaAs MESFET analytic theory for current-voltage characteristics and field distribution," *IEEE Trans. Electron Devices*, vol. ED-36, no. 2, pp. 281–288, Feb. 1989.
[22] A. Cappy *et al.*, "Noise modeling of submicrometer-gate two-dimensional electron-gate field-effect transistor," *IEEE Trans. Electron Devices*, vol. ED-32, no. 12, pp. 2787–2796, Dec. 1985.

Fullwave Analysis of Planar Microwave Circuits by Integral Equation Methods and Bilinear Transformations

Andreas Janhsen, Burkhard Schiek and Volkert Hansen

***Abstract*—Planar microwave circuits are simulated by a mixed space-spectral domain integral method which allows the consideration of space-varying impedances. For an efficient computation of scattering parameters of circuits containing lumped elements within this full wave analysis, a bilinear transformation is used. Furthermore, by this so-called Möbius transformation it is possible to decide whether an impedance region of finite size can be interpreted as a lumped element or not.**

I. Introduction

Since the early 80's there is an increasing interest in the investigation of planar microwave circuits based on a numerical solution of Maxwell's equations. These methods can be roughly devided into two groups:

The simulation of microwave circuits by finite differences (e.g., [1]), finite elements (e.g., [2]), by the transmission line method (e.g., [3]) and similar methods is advantageous for circuits with complicated shapes, because these techniques are based on a three-dimensional discretisation of the metallization of the circuit as well as of the dielectric structure. Lumped impedance elements, space varying conductivity and a finite thickness of the metallisation can be considered. However, an enormous numerical expense is necessary because of discretising in all three dimensions. Thus, these methods are mainly used for circuit simulations where the dimensions of the geometry are in the range of a wavelength. Radiation of the circuit into free space can only be considered approximately.

The second group includes the integral equation techniques (e.g., [4]–[6]) and in the broadest sense the method of lines [7]. Here, the three-dimensional discretization is reduced to a two-dimensional one. Therefore, the dielectric layers are described by their Green's function. The expenditure of analytical and program-technical preparation yields an efficient computation of the circuits for which the assumption of a plane layered dielectric environment is valid. Defining ideal electric or magnetic sidewalls surrounding the circuit, FFT algorithms (e.g. [8]) can be used advantageously. Finite conductivity and a finite thickness of the metallisation can be considered approximately defining a surface impedance. A method for the simulation of active and/or passive lumped elements within the integral equation techniques is described in [9]. This approach can be generalized to space-varying surface impedances [10].

The latter will be discussed in this paper. First a general model for circuits embedded in layered dielectric media will be introduced. Subsequently an integral equation technique of planar microwave circuits including space varying surface impedances is shortly outlined. The correlation of port-quantities, e.g., scattering parameters, and circuit terminals, e.g., lumped impedances, is created with the help of a bilinear transform. This leads to an efficient computation of scattering parameters of circuits containing lumped elements. Furthermore, it becomes possible to give a measure for the numerical validity of calculated scattering parameters and an indicator is definable, by which it can be decided whether an impedance region of finite size can be interpreted as a lumped element or not. By several examples the efficiency of this method is illustrated.

II. Model and Integral Equation

The multiport circuit which is to be analyzed is embedded in a layered dielectric medium (Fig. 1). By this model not only microstrip circuits with or without a superstrate but also stripline, coplanar and similar structures can be examined.

The surface current density $\vec{J}(x, y)$ on the metallic structure is represented by a sum over N piecewisely defined basis functions $f_n(x, y)$ with current amplitudes I_n:

$$\vec{J}(x, y) = \sum_{n}^{N} I_n \frac{f_n(x, y)}{b_n} \vec{u}_n, \tag{1}$$

where b_n is the width of the nth current mode. The number of basis functions depends on the complexity of the circuit.

The electric field has to fulfill the surface impedance boundary condition on the circuit (see e.g. [11]):

$$\vec{E}(x, y)|_{\tan} = Z_{\text{tot}}(x, y)\vec{J}(x, y) + \vec{E}^{\text{ex}}|_{\tan}. \tag{2}$$

The space-varying surface impedance consists of two parts

$$Z_{\text{tot}}(x, y) = Z_c + Z(x, y). \tag{3}$$

Thus, in addition to a finite conductivity Z_c which represents the overall conductor losses, we have a space-varying surface impedance $Z(x, y)$. By this space-varying surface impedance different kinds of metallisation can be modeled (e.g. a superconductive film) or/and we can model impedances of finite size or infinite small size. Introducing a Green's function of the stratified dielectric structure an integral equation can be obtained which is formulated in the spectral-domain as well as in the space-domain [9], [10]. Applying the method of moments we get the following set of linear equations:

$$\sum_{i}^{N} I_i(Z_{ji} - Z_{ji}^{xy}) = V_j \quad \text{with} \quad j = 1, \cdots, N + L. \tag{4}$$

$$Z_{ji} = \frac{1}{4\pi^2} \int_{k_y} \int_{k_y} \vec{u}_j (\overleftrightarrow{G}(k_x, k_y) - Z_c \overleftrightarrow{I}) \vec{u}_i \cdot \frac{F_i(k_x, k_y) F_j^*(k_x, k_y)}{b_i b_j} dk_x\, dk_y, \tag{5}$$

Manuscript received August 13, 1991; revised March 6, 1992.
The authors are with the Institut für Hochfrequenztechnik, IC6/134, Ruhr-Universität Bochum, 4630 Bochum, Germany.
IEEE Log Number 9200459.